Carbon Doping of the TiO_2 (110) Rutile Surface. A Theoretical Study Based on DFT

Jesús Graciani, Yanaris Ortega, and Javier Fdez. Sanz*

Departamento de Química Física, Facultad de Química, Universidad de Sevilla, E-41012 Sevilla, Spain

Received April 25, 2008. Revised Manuscript Received February 9, 2009

A detailed analysis of the structural and electronic properties of the C-doped rutile TiO_2(110) surface has been performed by means of periodic density-functional calculations. C atoms adsorb exothermically on the surface, although they are unstable with respect to the CO escape and formation of an oxygen vacancy. C implantation at lattice positions is an endothermic process, in contrast with what was observed in the case of N implantation. These C implanted atoms are also unstable in the presence of molecular oxygen. A strong cooperative interaction between implanted C atoms and surface oxygen vacancies is observed: (i) the presence of vacancies significantly lowers the implantation energy and stabilizes the C atoms, although not enough to avoid their escape in the presence of O_2; (ii) the presence of implanted C atoms noticeably lowers the energy of formation of oxygen vacancy in the surface. Finally, an analysis of the electronic structure confirms the presence of in-gap states that could improve the photocatalytic activity of rutile upon being doped with C.

1. Introduction

One of the challenges of the current scientific community concerns the search for efficient renewable energy strategies, because fossil fuels are nonrenewable and cause important environmental problems and it is not clear how long they will last. Among some plausible solutions, one of the most promising is to harvest the solar light and further conversion into other forms of energy or chemical reactions. After Fujishima's discovering that TiO_2 was able to photocatalytically split water to H_2 and O_2,[1] a great effort has been devoted to achieve improved efficiencies in photochemistry, photocatalysis and solar cells, using TiO_2 as semiconductor. In addition to the photoinduced decomposition of water, some other promising applications are water and air purifications by photodegradation of organic molecules[2−6] (which includes indoor air treatment, pollution treatments of aqueous or air affluents, remediation of underground water at polluted sites) and self-cleaning surfaces[7] and inactivation of bacteria and fungi.[8,9] Moreover, TiO_2 remains among the most promising materials for photocatalytic applications because of its low cost, chemical inertness, nontoxicity, and photostability. However, in spite of all these convenient properties, titanium dioxide has a serious drawback: it has a relatively wide band gap (3.0−3.2 eV) and adsorbs only a small proportion (∼5%) of solar light in the near-ultraviolet region.

To improve the photoactivity of TiO_2, researchers have considered both transition metal and nonmetal doping. However, transition-metal-doped materials[3,10−12] are thermally unstable,[10] tend to form charge carrier recombination centers, and require an expensive ion implantation facility.[11,12] Moreover, no noticeable change in band gap energy of TiO_2 was observed. Visible light absorption by the transition metal doped TiO_2 was found to be due to d−d transition of electrons in the transition metal dopants but not because of band gap lowering. The most promising materials that have been synthesized until now are non-metal-doped TiO_2. Since the pioneering work of Asahi,[13] nitrogen-doped TiO_2 has received a particular attention[14−20] because the implantation of nitrogen modifies the electronic structure by introducing localized states in the top of the valence band, narrowing the band gap. This reduction of the band gap makes possible the photocatalytic activity in a number of reactions under visible light.[13,21,22] In addition, highly efficient dye-sensitized

* Corresponding author. E-mail: sanz@us.es.

(1) Fujishima, A.; Honda, K. *Nature* **1972**, *238*, 37.
(2) Fox, M. A.; Dulay, M. T. *Chem. Rev.* **1993**, *93*, 341.
(3) Hoffmann, M. R.; Martin, S. T.; Choi, W.; Bahnemannt, D. W. *Chem. Rev.* **1995**, *95*, 69.
(4) Linsebigler, A. L.; Lu, G.; Yates, J. T. *Chem. Rev.* **1995**, *95*, 735.
(5) Robert, D.; Malato, S. *Sci. Total Environ.* **2002**, *291*, 85.
(6) Zhao, J.; Chen, C.; Ma, W. *Top. Catal.* **2005**, *35*, 269.
(7) Tryk, D. A.; Fujishima, A.; Honda, K. *Electrochim. Acta* **2000**, *45*, 2363.
(8) Mitoraj, D.; Janczyk, A.; Strus, M.; Kisch, H.; Stochel, G.; Heczko, P. B.; Macyk, W. *Photochem. Photobiol. Sci.* **2007**, *6*, 642.
(9) Agrios, A. G.; Pichat, P. *J. Appl. Electrochem.* **2005**, *35*, 655.
(10) Choi, W.; Termin, A.; Hoffmann, M. R. *J. Phys. Chem.* **1994**, *98*, 13669.
(11) Wang, Y.; Cheng, H.; Hao, Y.; Ma, J.; Li, W.; Cai, S. *Thin Solid Films* **1999**, *349*, 120.
(12) Anpo, M. *Catal. Surv. Jpn.* **1997**, *1*, 169.
(13) Asahi, R.; Morikawa, T.; Ohwaki, T.; Aoki, K.; Taga, Y. *Science* **2001**, *293*, 269.
(14) Qiu, X.; Burda, C. *Chem. Phys.* **2007**, *339*, 1.
(15) Beranek, R.; Neumann, B.; Sakthivel, S.; Janczarek, M.; Dittrich, T.; Tributsch, H.; Kisch, H. *Chem. Phys.* **2007**, *339*, 11.
(16) Nakano, Y.; Morikawa, T.; Ohwaki, T.; Taga, Y. *Chem. Phys.* **2007**, *339*, 20.
(17) Chambers, S. A.; Cheung, S. H.; Shutthanandan, V.; Thevuthasan, S.; Bowman, M. K.; Joly, A. G. *Chem. Phys.* **2007**, *339*, 27.
(18) Batzill, M.; Morales, E. H.; Diebold, U. *Chem. Phys.* **2007**, *339*, 36.
(19) Di Valentin, C.; Finazzi, E.; Pacchioni, G.; Selloni, A.; Livraghi, S.; Paganini, M. C.; Giamello, E. *Chem. Phys.* **2007**, *339*, 44.
(20) Asahi, R.; Morikawa, T. *Chem. Phys.* **2007**, *339*, 57.

10.1021/cm803436e CCC: $40.75
Published on Web 03/27/2009

solar cells have been obtained using nanocrystalline nitrogen-doped titania.[23]

However, C-doped TiO_2 has been found to be remarkably effective, even more than N-doped TiO_2.[24−31] In particular, Sakthivel and Kisch[26] found that C-doped TiO_2 is five times more active than N-doped TiO_2 in the degradation of 4-chlorophenol by artificial light ($\lambda \geq 455$ nm). Park et al.[27] reported that $TiO_{2-x}C_x$ nanotube arrays show much higher photocurrent densities and more efficient water splitting under visible light illumination than pure TiO_2 nanotube arrays. The total photocurrent was more than 20 times higher than that with P-25 nanoparticulate film under white light illumination. Kahn et al.[24] evaluated the photoresponse of C-doped TiO_2 by measuring the rate of water splitting to hydrogen and oxygen and found a photoconversion efficiencie as high as 8.35%. Chu et al. used C-doped TiO_2 as photoanode for solar cells, exhibiting high photocurrent densities and yielding an overall conversion efficiency of 4.42%.[29] Very recently, using C-doped TiO_2 under visible light, Mitoraj et al. achieved the inactivation of bacteria and fungi,[8] Cheng et al. observed the photocatalytic degradation of 4-chlorophenol[30] and Kuo et al. carried out the NO oxidation achieving up to 48% removal of NO_x.[31]

This excellent photobehavior of C-doped TiO_2 is attributed to a significant reduction of the band gap and to the appearance of some C states in the band gap (midgap band states). Experimentally, band gaps as narrow as 2.32,[24] 2.65,[28] or 2.78 eV[32] and midgap band values of around 1.4−1.5 eV[28,32] for C-doped TiO_2 have been found. Interestingly, Nakano et al. found three deep levels located at ∼0.86, ∼1.30, and ∼2.34 eV below the conduction band using deep-level optical spectroscopy.[33] They interpreted the first level was probably attributable to the intrinsic nature of TiO_2, whereas the other two levels were newly introduced by the C-doping. In particular, the pronounced 2.34 eV feature contributed to band gap narrowing by mixing with the O2p valence band. However, theoretical calculations have shown that substitutional and interstitial implanted C atoms generates three levels in the band gap, whereas C atom replacement of Ti atoms in the TiO_2 structure does not induce either gap states or band gap narrowing.[34−38] The deepest level is very near the O 2p edge and overlaps the valence band, whereas the two higher energy levels fall in the midband gap region. Moreover, from both theoretical and experimental viewpoints, it seems well-established that increasing the concentration of implanted C atoms induces larger photocatalytic activities by widening the midgap band.[35−37,39] According to previously published work, it turns out that visible light absorption is attributable to a significant narrowing of the band gap as well as to a complex midband in the band gap generated by a multiatom effect. The midgap band allows visible light absorption through electronic transitions to the conduction band and both electrons and holes are photocatalytically active.

On the other hand, it is well-known that TiO_2 surfaces, mainly the (110) rutile face, show a relatively high concentration of oxygen vacancies. There is a general agreement about that the highest energy level of C atoms is empty in the absence of oxygen vacancies and it is filled up in their presence. However, the role that oxygen vacancies and the in-gap levels play in the photocatalytic behavior of C-doped TiO_2 is controversial. Some authors found that oxygen vacancies improve photoactivity[40] while others proposed that they inhibit photocatalysis,[38] these differences being related to the proposed photocatalytic mechanisms.

With the exception of the preliminary work of Nie and Sohlberg,[34] previous theoretical analysis of C-doped TiO_2 has been performed by means of bulk calculations, in particular the work by Di Valentin et al.[37] The key role played by the surface structure in phenomena such as heterogeneous catalysis, as well as the stability of C implanted TiO_2 surfaces prompted us to perform a detailed analysis of the energetics and electronic structure of this material from periodic DFT calculations. One of our main aims was to study the stability of C-doped TiO_2 surfaces with respect to C escape (likely as CO). This process appears to be of great relevance as it opens the door to oxygen vacancies formation and thereby to deep surface reconstructions such as that observed when N is implanted on the TiO_2(110) surface, for which a massive rearrangement is observed.[41] The paper is arranged as follows. After describing the models and summarizing the computational details in section 2, the results are reported and discussed in section 3, which has been divided in four main items concerning C implantation on either a perfect surface or an O vacancy defective surface; the stability of implanted carbon in the presence of molecular oxygen and the analysis of the electronic structure are subsequently reported; and finally, the possible impact on the photocatalytic activity of the material is considered. Conclusions are outlined in section

(21) Chen, X.; Burda, C. *J. Phys. Chem. B* **2004**, *108*, 15446. Sathish, M.; Viswanathan, B.; Viswanath, R. P.; Gopinath, C. S. *Chem. Mater.* **2005**, *17*, 6349. G. R. Torres, G. R.; Lindgren, T.; Lu, J.; Granqvist, C.-G.; Linquist, S.-E. *J. Phys. Chem. B* **2004**, *108*, 5995. Belver, C.; Bellod, R.; Stewart, S. J.; Requejo, F. G.; Fernández-García, M. *Appl. Catal., B* **2006**, *65*, 309.
(22) (a) Nakamura, R.; Tanaka, T.; Nakato, Y. *J. Phys. Chem. B* **2004**, *108*, 10617. (b) Mrowetz, M.; Balcerski, W.; Colussi, A. J.; Hoffmann, M. R. *J. Phys. Chem. B* **2004**, *108*, 17269.
(23) Ma, T. L.; Akiyama, M.; Abe, E.; Imai, I. *Nano Lett.* **2005**, *5*, 2543.
(24) Khan, S. U. M.; Al-Shahry, M.; Ingler, W. B., Jr. *Science* **2002**, *297*, 2243.
(25) Khan, S. U. M.; Al-Shahry, M.; Ingler, W. B., Jr. *Science* **2003**, *301*, 1673.
(26) Sakthivel, S.; Kisch, H. *Angew. Chem., Int. Ed.* **2003**, *42*, 4908.
(27) Park, J. H.; Kim, S.; Bard, A. J. *Nano Lett.* **2006**, *6*, 24.
(28) Shaban, Y. A.; Kahn, S. U. M. *Chem. Phys.* **2007**, *339*, 73.
(29) Chu, D.; Yuan, X.; Qin, G.; Xu, M.; Zheng, P.; Lu, J.; Zha, L. *J. Nanopart. Res.* **2007**, DOI 10.1007/s11051−007−9241−7.
(30) Cheng, Y.; Sun, H.; Jin, W.; Xu, N. *Chem. Eng. J.* **2007**, *128*, 127.
(31) Kuo, Ch.-Sh.; Tseng, Y.-H.; Huang, Ch.-H.; Li, Y.-Y. *J. Mol. Catal. A: Chem.* **2007**, *270*, 93.
(32) Xu, C.; Killmeyer, R.; Gray, M. L.; Kahn, S. U. M. *Appl. Catal. B: Environ.* **2006**, *64*, 312.
(33) Nakano, Y.; Morikawa, T.; Ohwaki, T.; Taga, Y. *Appl. Phys. Lett.* **2005**, *87*, 052111.
(34) Nie, X.; Sohlberg, K. *Mater. Res. Soc. Symp. Proc.* **2004**, *801*, BB6.6.1.
(35) Wang, H.; Lewis, J. P. *J. Phys.: Condens. Matter* **2005**, *17*, L209.
(36) Wang, H.; Lewis, J. P. *J. Phys.: Condens. Matter* **2006**, *18*, 421.
(37) Di Valentin, C.; Pacchioni, G.; Selloni, A. *Chem. Mater.* **2005**, *17*, 6656.
(38) Kamisaka, H.; Adachi, T.; Yamashita, K. *J. Chem. Phys.* **2005**, *123*, 084704.
(39) Xu, C.; Khan, S. U. M. *Electrochem. Solid-State Lett.* **2007**, *10*, B56.
(40) Li, Y.; Hwang, D.-S.; Lee, N. H.; Kim, S.-J. *Chem. Phys. Lett.* **2005**, *404*, 25.
(41) Batzill, M.; Morales, E.; Diebold, U. *Phys. Rev. Lett.* **2006**, *96*, 026103.

4. All through the discussion, the results are compared with those we reported for N-doped TiO_2 (110) using a similar approach. We found such a comparison of major interest as we observed that in general C implantation is more unstable than that of N. Also, adsorption on top of bridge oxygen atoms leads to spontaneous escape of CO leaving a vacancy behind, and therefore, surface reconstructions would be expected to happen even easier than when N is implanted. This would agree with some experimental results that suggest that after C doping, TiO_2 surfaces are more porous[24,29] and rougher.[28]

2. Model and Computational Procedures

To model the extended nature of these surfaces, periodic three-dimensional (3D) DFT calculations were carried out using the VASP 4.6 code[42,43] with the projector augmented wave method (PAW).[44] In these calculations, the energy was obtained using the GGA implementation of DFT proposed by Perdew et al.[45] and the electronic states were expanded using plane waves as a basis set with a cutoff of 400 eV. In the case of Ti atoms, besides the valence 4s and 3d electrons, the 3s and 3p semicore states were also explicitly included in the calculations. To obtain faster convergence with respect to the number of k points thermal smearing of one-electron states ($k_BT = 0.05$ eV) has been allowed using the Gaussian smearing method to define the partial occupancies. Energy was sampled on a $2 \times 4 \times 1$ grid generated using the Monkhorst-Pack method. The number of k points was selected in order to get TS corrections to the energy less than 0.001 eV/atom together with negligible changes in the optimized cell parameters. Forces on the ions were calculated through the Hellmann-Feyman theorem as the partial derivatives of free energy with respect to the atomic position, including the Harris-Foulkes[46] correction to forces. This calculation of the forces allows a geometry optimization using the conjugate-gradient scheme. Iterative relaxation of atomic positions was stopped when the change in total energy between successive steps was less than 0.001 eV. With this criterion, forces on the atoms generally were less than 0.05 eV/Å.

To describe the surface, we used the same surface slab model successfully used in a previous work.[47] Essentially, the model consists of six Ti-layers (18 atomic layers) and a vacuum space of 10 Å between the slabs. The four outermost layers are allowed to relax while the remaining deepest layers are kept fixed at the optimized atomic bulk positions. The main advantage of this model is to avoid spurious effects due to the finite thickness of the slab[48,49] as it minimizes the well-known energy oscillations as a function of the number of layers (even−odd) and reaches convergence for both the geometric and electronic surface structures. The size of the surface model is (4×1), which is adequate to represent both carbon and vacancy concentrations, the final number of atoms in the supercell being 144. Lastly, to avoid artifacts in the electronic structure derived from the nonrelaxed atoms, the density of state (DOS) calculations have been computed from fully relaxed structures, using the tetrahedron method with Bloch corrections and a k-point grid enlarged to $4 \times 8 \times 2$.

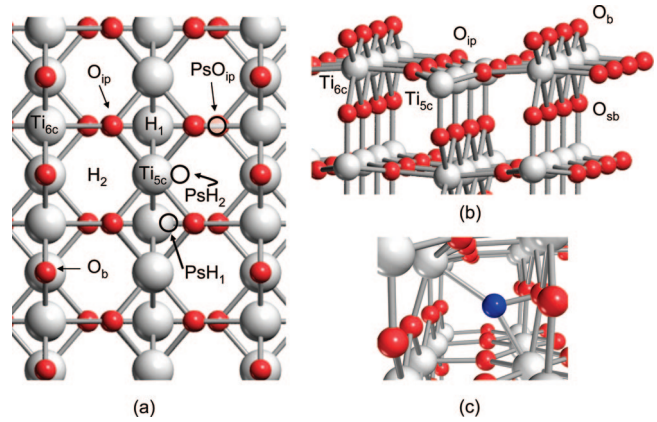

Figure 1. Adsorption sites on the TiO_2 (110) rutile surface. (a) Top view, (b) side view, (c) interstitial site.

In our simulations of C implantation we take as both reference and initial state C(g), as triplet, ^3P, so we can wonder about the spin state of the final product. To clarify this point we ran preliminary calculations that showed that after C adsorption on the TiO_2 rutile surface there is a spin quenching and the spin nonpolarized solution is 0.13 eV more favorable that the spin polarized one. On the basis of this result, the energetics we report are based on spin nonpolarized calculations with the exception of C atom (^3P) and molecular oxygen ($^3\Sigma_g^-$), which are computed as triplets. Notice on the other hand that the choice of references is arbitrary and we could have taken a different one, the effect only being an additive constant. For instance, if the reference for C were graphite, all the adsorption and substitution energies should be shifted by 8.05 eV.

3. Results and Discussion

3.1. Carbon Implantation on a Perfect Surface. We start this section describing the labeling used in this work (see Figure 1). Bridging oxygen atoms are labeled O_b when they are above the uppermost Ti plane. If they are at the same level they are called in plane, O_{ip}, and if they are under this level they are called sub-bridge, O_{sb}. Vacancies and substitutional nitrogen/carbon inherit the same nomenclature. We use a superscript to indicate the layer to which they belong, the uppermost layer being the number one. On the surface, there are two types of Ti cations that are labeled as Ti_{6c} and Ti_{5c} for the hexa-coordinated and penta-coordinated ones, respectively. Notice that the label Ti_{6c} refers to the atom perpendicularly lying down the surface, although the main interaction takes with a pair of bridging oxygens. In addition to the lattice adsorption atop sites, there are five possible hollow positions labeled H1, H2, PsH1, PsH2, and PsO_{ip} as indicated in Figure 1. On the other hand, there are two different ways for C to implant on the TiO_2 (110) rutile surface, namely pure adsorption (both on surface and interstitial sites) and substitution of an lattice oxygen by a C atom.

3.1.1. Implantation by Adsorption. C adsorption energies, E_{ad}^{C}, for the different sites were computed using the following formulas

(42) Kresse, G.; Hafner, J. *Phys. Rev. B* **1993**, *47*, R558.
(43) (a) Kresse, G.; Furthmuller, J. *Comput. Mater. Sci.* **1996**, *6*, 15. (b) Kresse, G.; Furthmuller, J. *Phys. Rev. B* **1996**, *54*, 11169.
(44) Kresse, G.; Joubert, J. *Phys. Rev. B* **1999**, *59*, 1758.
(45) Perdew, J.; Chevary, J.; Vosko, S.; Jackson, K.; Pederson, M.; Singh, D.; Fiolhais, C. *Phys. Rev. B* **1992**, *46*, 6671.
(46) (a) Harris, J. *Phys. Rev. B* **1985**, *31*, 1770. (b) Foulkes, W. M. C.; Haydock, R. *Phys. Rev. B* **1989**, *39*, 12520.
(47) Graciani, J.; Álvarez, L. J.; Rodríguez, J. A.; Sanz, J. F. *J. Phys. Chem.* **2008**, *112*, 2624.
(48) Hameeuw, K. J.; Cantele, G.; Ninno, D.; Trani, F.; Iadonesi, G. *J. Chem. Phys.* **2006**, *124*, 024708.
(49) Thompson, S. J.; Lewis, S. P. *Phys. Rev. B* **2006**, *73*, 073403.

$$C(g) + TiO_2 \rightarrow TiO_2C_{ad}$$

$$E_{ad}^{C} = E(\text{surface with adsorbed C}) - E(\text{surface}) - E(C(g))$$

where C_{ad} is the adsorbed C atom and the reference is an isolated gas phase C atom with energy $E(C(g))$. Table 1 summarizes the results of these calculations and Figure 2 shows the optimized geometry for the most relevant structures. As can be seen, adsorption is always exothermic with values as large as −4.03 eV for the most stable site Ti_{6c}. This is in contrast with the results computed for N doping where the adatom-surface interaction was found to be significantly lower and in some cases the process also was endothermic. With the exception of Ti_{5c} site (the less stable and actually a metastable position) adsorbed C tend to form CO or CO_2 like species, with CO distances ranging between 1.25 and 1.57 Å. In fact, there is a nice correlation between the CO distances and the strength of the C−surface interaction. Site Ti_{6c} seems to be an exception, although in this case, the C atom binds two O_b atoms forming a CO_2-like species (with relatively short C−O distances, 1.33 Å); in fact, this is the most stable adsorption site. As can be seen in Figure 2c−d, the CO_2-like structure appears strongly bent and consequently the C atom should be oxidized. A Bader analysis for this structure gives for the C atom a net charge of +1.98 |e| in agreement with the expected formal value of +2. Adsorption on PsH2 also involves interaction with two oxygen atoms, although the main bond is with the metal and the adsorption energy results ∼2 eV smaller. This is in contrast with PsH1 site: two C−M and one C−O raises to 3.32 eV. The difference between sites PsH2 and PsH1 can be traced through both the C−O distances, 1.51 and 1.33 Å, respectively, and the C−M ones, 1.97 and 2.17 Å, respectively. As a result, the adsorption energy on PsH1 (in which the short C−O bond is the main bond) is 1.3 eV larger than PsH2 (in which the two large C−O bonds are secondary). Adsorption at PsO_{ip} seems also to be controversial as the C−O distance is really short (1.25 Å) but the interaction energy is one of the smallest found. In this case, though the adsorbed C strongly binds an O_{ip} atom, it strongly feels the repulsion of the two bridge oxygen O_b atoms, which actually leads to a large distortion around the site.

On the other hand, it is worth noting that we were not able to find a stationary point when the C atom was placed on top of an O_b atom. Instead, formation and further desorption of a CO molecule was observed. In other words, an oxygen vacancy at the bridge site is spontaneously generated in the (110) surface of rutile each time a C atom interacts with a bridge oxygen atom. Furthermore, this result suggests a potential instability of adsorbed C_{ad} atoms with respect to an eventual escape as CO. To check this possibility, the energy involved in the escape of the adsorbed C_{ad} atoms as CO, leaving an oxygen vacancy behind in the surface structure, was estimated for the other sites. These

Table 1. Adsorption Energies (eV); C−O and C−Ti Bond Distances (Å), and CO(g) Escape Energies for C Atoms Adsorbed on the Surface[a]

	adsorption energies (eV)		distances (Å)			
adsorption site	C(g)	N(g)	C−O	C−Ti_{5c}	C−Ti_{6c}	CO escape leaving behind a vacancy
O_b	**CO escape**	−1.39	**1.15** (1)			**spontaneous**
O_{ip}	PsH_1	−0.82				
PsO_{ip}	−2.46	O_{ip}	1.25 (1)		2.28	−1.18 (V_{ip})
Ti_{5c}	−0.17	0.72		2.04		
Ti_{6c}	−4.03	0.10	1.33 (2)		2.49	−1.44 (V_b)
H_1	−3.19	−0.34	1.57 (2)	2.13		−0.45 (V_{ip})
PsH_1 (MMO)	−3.32	−1.33	1.33 (1)	2.17		−0.32 (V_{ip})
PsH_2 (OOM)	−2.03	0.54	1.51 (2)	1.97		−1.61 (V_{ip})
interstitial	−3.41	−1.03	1.26 (1)	2.21	2.11	−1.71 (V_{sb})
CO			1.13			
CO_2			1.16			

[a] Values of N are shown as reference for comparison. CO and CO_2 bond distances given at the bottom are experimental values. Between parentheses are the number of oxygen atoms bound to the C atom.

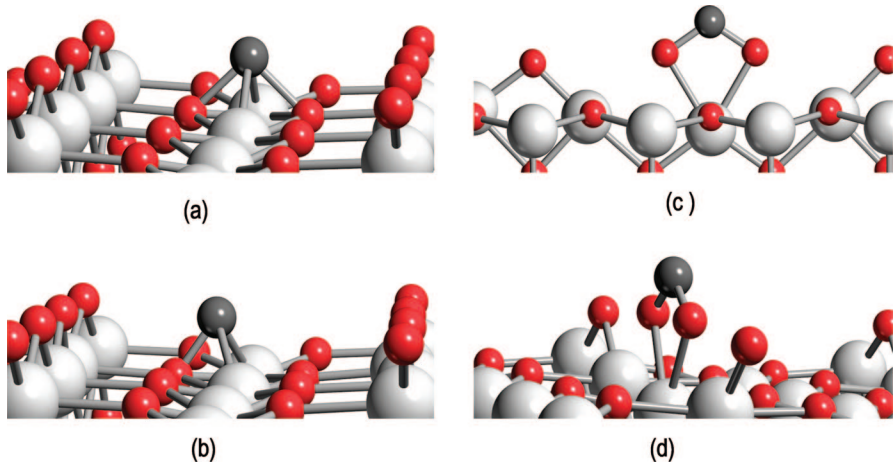

Figure 2. Some relevant optimized structures of C adsorbed on the TiO_2 (110) surface. (a, b) H1 and PsH1 sites; (c, d) CO_2-like structure obtained when C interacts at site Ti_{6C} with two bridging oxygen atoms.

energies, estimated according to

$$TiO_2C_{ad} \rightarrow TiO_{2-x} + xCO$$

$$E^{CO}_{esc,C_{ads}} = E(\text{surface with the oxygen vacancy}) + E(CO(g)) - E(\text{surface with adsorbed C})$$

are also reported in Table 1. Indeed, it is really interesting to confirm that CO escape with formation of a surface oxygen vacancy is always exothermic. This finding indicates that the earliest stages of the C adsorption will involve a strong reduction of the TiO_2 (110) rutile surface via vacancy formation. Because the escape of N as NO leaving a vacancy at the bridge position was found to be endothermic by 0.35 eV,[47] C adsorption is expected to induce surfaces reconstructions even larger than in the case of N implantation.[41] Two more comments are worth mentioning at this point. First that this analysis nothing says about the possible barriers involved in the formation and further distortion of the substrate to make way to CO to leave. It is easily conceivable that for an interstitial C to leave, a high barrier must be in place. The second point concerns the apparent contradiction between the spontaneous escape of CO when C adsorbs at bridging oxygen atoms with the experimentally observed adsorption of CO on TiO_2 surfaces.[50,51] Indeed, it has been shown that CO weakly interacts with stoichiometric titania surfaces and the interaction becomes stronger when the surface is reduced. However, it should be noticed that such an adsorption involves CO molecules bonding to the surface through the C atom.[50,52]

3.1.2. Implantation by Substitution. Energies necessary to implant a C atom by substitution of a lattice O atom were calculated according to

$$C(g) + TiO_2 \rightarrow TiO_{2-x}C_x + \frac{x}{2}O_2(g)$$

$$E_{imp} = E(\text{surface with implanted C}) + \frac{1}{2}E(O_2(g)) - E(\text{surface}) - E(C(g))$$

As can be seen in Table 2, the implantation process is endothermic whatever the site is. This is in contrast with the results obtained in the case of N implantation where some sites were found to be stabilized. In general it is found that substitution is easier on the bulklike sites of the second layer, the ordering being $C^2_b > C_{sb} > C^2_{ip} \geq C^2_{sb} > C_{ip} > C_b$.

3.2. Carbon Implantation on Surfaces with Vacancies. The reactivity of TiO_2 (110) is highly dependent on oxygen vacancies, which on the other hand constitute the most common defect on the rutile surface.[53−55] The most widespread vacancy is that corresponding to the bridging oxygen atoms, V_b, with a concentration usually around 7−10% with respect to bridging oxygen atoms.[54,56] Furthermore, under certain conditions, there are migrations of vacancies from the bulk to the surface.[57−59] At a first stage, the presence of vacancies in the surface leads one to think of the adsorption of C(g) in these defects, which after C covering would give C atoms as part of the lattice structure, i.e., structures identical to those obtained by substitution. The process can be described as

$$TiO_{2-x}Vac + xC(g) \rightarrow TiO_{2-x}C_x$$

where Vac accounts for oxygen vacancies. The energetics associated to the process is computed using

$$E^{\text{at V}}_{imp} = E(\text{Surf. with implanted C}) - E(\text{Surf. with vacancy}) - E(C(g))$$

and the results are also reported in Table 2. Notice that the final states in this process are the same as those obtained from a pure O substitution on a perfect surface. They differ in the initial states that here correspond to vacancies at different sites. The energies of vacancy formation are also given in Table 2 and the way they are estimated is explained below. As can be seen in Table 2, the implantation is highly exothermic in all sites and therefore a full coverage of vacancies is expected. However, when these energies are compared with those reported in Table 1 that correspond to the adsorption step, it turns out that pure adsorption on some sites would be preferred. For instance, although the interaction energy at the Ti_{6c} site is −4.03 eV, implantation at a V_b vacancy would release only −2.09 eV. We can wonder, however, if the filling rate of vacancies is too high as it involves incorporation of a C atom each supercell. To check this point, we performed a series of calculations with a supercell doubled, always six layers thick: $4 \times 2 \times 6$. With this model, the energy release values are −2.81 eV for the first vacancy and −1.13 eV for the second. Notice that the mean value, −1.97 eV, is nearly the same as for the smaller cell (−2.09 eV). In any case, taking just the value for the first implantation, −2.81 eV, it still falls far from that of a pure adsorption (−4.03 eV at the Ti_{6c} site), and therefore, assuming that the adsorption energies remain unchanged in the presence of a vacancy, C atoms reaching the surface would preferentially adsorb rather than fill V_b vacancies. Moreover, these results are in contrast with those found for N implantation, for which the vacancies were clearly the preferential sites for N incorporation.

Let us now analyze the interaction C-vacancy. The energetics related to the formation of oxygen vacancies and their relative stability have been analyzed in a number of papers and the subject still is open as the estimates show

(50) Linsebigler, A.; Lu, G.; Yates, J. T., Jr. *J. Chem. Phys.* **1995**, *103*, 9438.
(51) Lisachenko, A. A.; Mikhailov, R. V.; Basov, L. L.; Shelimov, B. N.; Che, M. *J. Phys. Chem. C* **2007**, *111*, 14440.
(52) For theoretical work see: (a) Scaranto, J.; Giorgianni, S. *J. Mol. Struct. (THEOCHEM)* **2008**, *858*, 72, and references therein.
(53) Henrich, V. E.; Cox, P. A. *The Surface Science of Metal Oxides*; Cambridge University Press: Cambridge, U.K., 1996.
(54) Diebold, U. *Surf. Sci. Rep.* **2003**, *48*, 53.
(55) Rasmussen, M. D.; Molina, L. M.; Hammer, B. *J. Chem. Phys.* **2004**, *120*, 988.
(56) Hebenstreit, E. L. D.; Hebestreit, W.; Diebold, U. *Surf. Sci.* **2001**, *470*, 347.
(57) Rodriguez, J. A.; Jirsak, T.; Liu, G.; Hrbek, J.; Dvorak, J.; Maiti, A. *J. Am. Chem. Soc.* **2001**, *123*, 9597.
(58) Jug, K.; Fair, N. N.; Bredow, T. *Phys. Chem. Chem. Phys.* **2005**, *7*, 2616.
(59) Hebenstreit, E. L. D.; Hebestreit, W.; Geisler, H.; Ventrice, C. A., Jr.; Sprunger, P. T.; Diebold, U. *Surf. Sci.* **2001**, *486*, L467.

strong dependence on the model used.[60,61] The energy needed to form oxygen vacancies in the perfect TiO_2 (110) rutile surface, E_f^V, according to the formula

$$E_f^V = 1/2E(O_2\ \text{molecule}) + E(\text{surface with a vacancy}) - E(\text{surface})$$

was estimated to be 3.29 eV for the most favored site, the bridge oxygen, V_b using the $4 \times 1 \times 6$ supercell in agreement with the accepted value of ~3 eV.[61] The values associated to the different sites and layers have been reported for this model in reference.[47] In its turn, the energy needed to form a vacancy V_b when there is a C_{imp} atom, $E_f^{V_b}(C_{imp})$, is estimated as

$$E_f^{V_b}(C_{imp}) = 1/2E(O_2(g)) + E(\text{surface with a } V_b \text{ and a } C_{imp}) - E(\text{surface with a } C_{imp})$$

The results of these calculations are reported in Table 2. Compared to that corresponding to the pristine surface (3.29 eV), we can see that there is a dramatic and general lowering in the vacancy formation energies $E_f^{V_b}(C_{imp})$, with values as low as 1.23−1.61 eV when the C atom is implanted in the second layer. This behavior agrees with that observed in the case of N implantation, where the energy of vacancy formation dropped to 1.49 eV[47] and a similar reduction has also been observed for the bulk of C-doped TiO_2, both rutile and anatasa polymorphs.[37] The evidence of a strong interaction between carbon and oxygen vacancies may also be viewed from the other side, as the previous existence of a V_b significantly lowers the implantation energy, whatever is the site. As reported in Table 2, the energies for C implantation by substitution, $E_{imp}^{V_b}$, become negative, i.e., exothermic, when there is a vacancy at the bridging O site (V_b). There is, however, an exception when the carbon atom replaces a bridging oxygen atom for which the process still remains slightly endothermic (0.13 eV).

3.3. Stability in the Presence of Molecular Oxygen. As an additional test of the stability of the implanted C, we also estimated the energy necessary to remove carbon from the structure as CO(g) in the presence of O_2(g). These energies are computed according to

$$TiO_{2-x}C_x + \frac{x}{2}O_2(g) \rightarrow TiO_{2-x} + xCO(g)$$

$$E_{esc} = E(\text{surface with vacancy}) + E(CO(g)) - E(\text{surface with implanted C}) - \frac{1}{2}E(O_2(g))$$

These values together with those computed for the escape of NO are reported in Table 3. As can be seen, the energy associated to the escape of implanted carbon, C_{imp}, is negative and even larger (in absolute value) than in the case of adsorbed carbon atoms C_{ad}, reported in Table 1. The process is thermodynamically favored whatever the site is with large releases of energy (3.48−6.67 eV). This result is of major interest taking into account that such an escape of CO leaves an oxygen vacancy behind. In contrast, the escape of NO is mostly endothermic, with the exception of the bridge and sub-bridge sites, whose values are moderately negative. The difference between these two processes (roughly 5 eV) may not be attributed only to the difference of the CO and NO bond strengths. Actually, if we take as reference the escape of N_{imp} as 1/2 N_2(g), although the N−N bond is stronger than the N−O one, there are still two sites in which the escape remains endothermic (Table 3). This result confirms again what was shown above in the sense that C_{imp} atoms are significantly more unstable than the N_{imp}. In other words, it seems that rutile TiO_2 accepts better N atoms than C ones in its structural lattice positions. Because only low concentrations (3−5%) of implanted N can be reached experimentally,[41,62] even lower concentrations are expected for implanted C in the presence of O_2. Also, as concluded in the case of C adsorption, the larger instability of substitutional C with respect to N suggests a deeper surface reconstructions.

The instability of implanted C atoms in the presence of oxygen seems to be corroborated by some experimental findings which show that implanted C atoms are not stable either when the temperature is raised, or in the presence of air.[28,31,63] For instance, the implantation of C at 500 °C in absence of oxygen leads to a C concentration of 22.2%. However, at the same temperature, if oxygen is present, the reached concentration was 5.63%. Similarly, in the absence

Table 2. Carbon Implantation Energies (eV) through Oxygen Substitution at Different Sites of the TiO_2 (110) Rutile Surface[a]

	perfect surface		surface with vacancies		
$site_{imp}$	E_{imp}	E_f^V	$E_{imp}^{V_b}$	$E_{imp}^{at\ V}$	$E_f^{V_b}(C_{imp})$
O_b	1.20	3.29	0.13	−2.09	2.42
O_{ip}	0.81	5.12	−0.90	−4.30	1.58
O_{sb}	0.47	3.64	−0.96	−3.17	1.86
O_b^2	0.19	5.48	−1.75	−5.28	1.35
O_{ip}^2	0.56	4.89	−1.12	−4.34	1.61
O_{sb}^2	0.58	5.28	−1.48	−4.70	1.23

[a] The initial state of the surface can be either a perfect surface, E_{imp}, or a surface with a bridge oxygen vacancy, $E_{imp}^{V_b}$. The energy of vacancy formation for the perfect surface is E_f^V, whereas $E_f^{V_b}(C_{imp})$ is the energy needed to create a bridge oxygen vacancy when a C atom is implanted at a given site of the lattice. $E_{imp}^{at\ V}$ stands for the energy released when the implantation is done by adding a C atom to the surface with a vacancy at that site.

Table 3. Escape Energies, E_{esc} (eV), of Implanted C as CO in the Presence of Molecular Oxygen for the Different Sites of the C-TiO_2 Doped Surfaces[a]

	perfect surface E_{esc}			surface with O_b vacancy E_{esc}
$site_{imp}$	CO	NO	1/2 N_2	CO
O_b	−6.67	−1.24	−2.24	−4.04
O_{ip}	−4.45	0.92	−0.08	−2.56
O_{sb}	−5.59	−0.50	−1.50	−2.43
O_b^2	−3.48	1.57	0.57	−1.39
O_{ip}^2	−4.42	0.81	−0.19	−2.43
O_{sb}^2	−4.06	1.25	0.25	−2.00

[a] Left values are those for a perfect surface, whereas the right column corresponds to a surface with a vacancy at the bridge oxygen site. Similar energies for the escape of NO and N_2 are also shown.

(60) Oviedo, J.; San Miguel, M. A.; Sanz, J. F. *J. Chem. Phys.* **2004**, *121*, 7427.
(61) Ganduglia-Pirovano, M. V.; Hofmann, A.; Sauer, J. *Surf. Sci. Rep.* **2007**, *62*, 209.
(62) Nambu, A.; Graciani, J.; Rodríguez, J. A.; Wu, Q.; Fujita, E.; Sanz, J. F. *J. Chem. Phys.* **2006**, *125*, 094706.
(63) Xu, C.; Killmeyer, R.; Gray, M. L.; Kahn, S. U. M. *Electrochem. Commun.* **2006**, *8*, 1650.

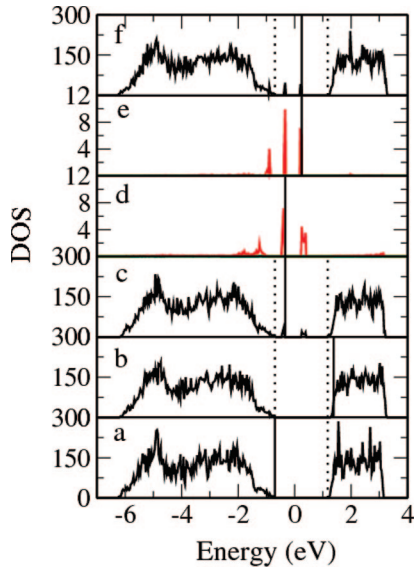

Figure 3. Density of state (DOS) plots: (a) total DOS for stoichiometric perfect TiO_2 (110) rutile surface; (b) total DOS with a bridge oxygen vacancy; (c) total DOS with an implanted C atom; (d) same as c, but projected on the C atom. The top two panels correspond to the surface bearing both vacancy and implanted C atom: (f) total DOS and (e) projected on C. Vertical lines show (solid lines) the top of the valence band for each system and (dotted lines) the band gap of stoichiometric pure TiO_2.

of oxygen, when the temperature is elevated to 900 °C, the reached concentration is 14.2%.[31] Moreover, Shaban and Khan pointed out in a recent work that if the temperature or oxidation time is too high, carbon atoms are removed from the sample.[28]

Finally, although as stated above, oxygen vacancies facilitate the implantation of C atoms, one can wonder whether or not such stabilization is large enough to avoid the escape of C as CO in the presence of oxygen. The energies of C escape as CO reported in Table 2 show that the presence of the oxygen vacancies lowers by 2−3 eV the absolute values of the energies of CO escape, although the escaping process still remains strongly exothermic.

3.4. Electronic Structure. The origin of the strong C-vacancy interaction may be explained through the analysis of the electronic density of states (DOS). Figure 3 shows the DOS for all four systems considered, namely the perfect pure surface, the surface with one oxygen vacancy in the bridge position (V_b), the surface with one implanted C atom, and the surface with both implanted C and oxygen vacancy (C+V). Some significant projections are also displayed. As can be observed the valence band maximum, VBM, features noticeable changes from one system to another, obviously due to deep changes in the electronic structure. Pure and perfect TiO_2 is an insulator. The formal oxidation state of oxygen is O^{2-} and therefore it has the O 2p band full. The metal oxidation state, Ti^{4+}, implies that Ti 3d band is formally empty. The calculated energy band gap is ∼2.0 eV (Figure 3a), which is, as usual, underestimated by DFT-GGA (experimental ∼3.0 eV[64]), in agreement with previous work.[65] In the case of TiO_2, DFT hybrid functionals including exchange (B3LYP) have been shown to correctly estimate the band gap.[66,67] Also the use of the DFT+U (Hubbard parameter) approximation has been shown to be a useful tool in describing the electronic structure of reduced TiO_2.[68] However, as we shall see in what follows, this inaccurate description of the band gap does not affect the qualitative description of the electronic interaction between carbon atoms and oxygen vacancies.

In the nonstoichiometric surface (Figure 3b), the nature of the top of the valence band is qualitatively different. The removal of a bridging oxygen atom leaves two electrons that start filling the Ti3d band, reducing the oxidation state of metallic atoms in the vicinity of the vacancy from Ti^{4+} to Ti^{3+} as experimentally observed.[62,69] On the other hand, as can be seen in Figure 3c, when an oxygen atom from the stoichiometric surface is substituted by a carbon atom, new small features appear in the band gap. The nature of such features may be ascertained if we consider the projection of the density of states over the C atom, shown in Figure 3d. As can be seen, the C atom shows two 2p tiny localized states just in the same positions than those of the total DOS, and one more mixed with the top of the O2p band. These states are located at 1.10, 1.73, and 2.56 eV below the minimum of the conduction band, in qualitative agreement with the experimental values (0.86, 1.30−1.50, and 2.32−2.78 eV[24,28,32,33]) and previous theoretical.[34−38] Further inspection of these C2p states shows that they are partially occupied corresponding to a formal C oxidation state of −2 and, therefore, some empty states above the Fermi level still are present.

When both vacancies and C atoms are present, electrons will move from the higher 3d occupied states (vacancy, Ti^{3+}) to the lower energy empty 2p states (C^{2-} impurities). This process means that the C^{2-} ion transforms into C^{4-} filling up the C 2p band. Formally, every C atom is able to oxidize two Ti^{3+} ions to Ti^{4+}, thus fully compensating an oxygen vacancy. This is contrast with N implantation, where two N atoms are needed to trap the electron pair of the vacancy. The process can be observed in Figure 3f where the top of the valence band now appears just above the C2p band, and is similar to the electron trapping observed by Di Valentin et al. in the carbon doping of bulk rutile.[37] This double electron shift and its concomitant stabilization explains three fundamental facts: (1) the easiness to form oxygen vacancies when implanted C is present, (2) the easiness to implant C when oxygen vacancies are present, and (3) the lowering of the exothermicity associated with the escape of C as CO, in the presence of molecular oxygen, when vacancies are present. The position of the C 2p bands are slightly shifted and are now located at 0.95, 1.49, and 2.08 eV, below the minimum of the conduction band, again in qualitative agreement with the experiment.[33]

(64) Henrich, V. E.; Kurtz, R. L. *Phys. Rev. B* **1981**, *23*, 6280.
(65) Di Valentin, C.; Pacchioni, G.; Selloni, A. *Phys. Rev. B* **2004**, *70*, 085116.
(66) Muscat, J.; Wander, A.; Harrison, N. M. *Chem. Phys. Lett.* **2001**, *342*, 397.
(67) Di Valentin, C.; Pacchioni, G.; Selloni, A. *Phys. Rev. Lett.* **2006**, *97*, 166803.
(68) Calzado, C. J.; Hernández, N. C.; Sanz, J. F. *Phys. Rev. B* **2008**, *77*, 045118.
(69) Livraghi, S.; Paganini, M. C.; Giamello, E.; Selloni, A.; Di Valentin, C.; Pacchioni, G. *J. Am. Chem. Soc.* **2006**, *128*, 15666.

3.5. Consequences on the Photocatalytic Activity of TiO_2 Rutile. The present analysis suggests that there is a noticeable difference in the expected experimental photocatalytic behavior between N and C implanted systems. As shown in our previous work.[47] N implantation in rutile surface is not expected to improve the photocatalytic efficiency of TiO_2 because no band gap reduction is actually observed. Indeed, the N 2p empty states initially are located above the valence band, but when occupied, they move downward and overlap the O2p band of the solid with a large stabilization.

However, when the in-gap 2p states of the implanted C are filled, they remain in the band gap. Although the photoactivity of such states compared to those arising from band-to-band transitions is uncertain, it is expected that C-doped TiO_2 rutile will show some improvement in its photocatalytic behavior. These states may be related to the experimentally found midgap states, which enhances the visible light absorption by transitions of electrons to the conduction band.[34] This process generates holes in the C impurity levels and electrons in the conduction band. Electrons are expected to have higher mobility than trapped holes, but it is not a drawback because direct interactions between trapped holes and adsorbed molecules have been observed experimentally.[70] Without vacancies, the visible light absorption is also likely but by electronic transitions from the valence band to unoccupied in-gap impurity bands.[38] In this case, the process generates holes in the valence band and electrons trapped in the in-gap impurity levels. As in the previous case, although holes are expected to have higher mobility than trapped electrons, that trapping is not expected to avoid the photocatalytic reaction with adsorbed molecules. Moreover, besides the presence of C in-gap states, the relative stabilization of vacancies at the surface might increase its activity in both adsorption processes and surface reactions.

(70) Liu, H.; Imanishi, A.; Nakato, Y. *J. Phys. Chem. C* **2007**, *111*, 8603.

4. Conclusions

We report on a theoretical DFT study of the C implantation process in the TiO_2 (110) rutile surface using a periodic slab surface model. Several scenarios for C implantation such as adsorption/substitution on both perfect and defective surfaces have been considered. Adsorption of C on both surface and interstitial sites is exothermic although a neat trend to recombine with surface oxygen atoms and escape as CO leaving a vacancy behind is found. This finding indicates that C deposition on the surface will induce significant surface reduction and likely surface reconstruction. This is in agreement with the experimental roughness observed upon C adsorption. C implantation by substitution of surface O atoms is an endothermic process and in the presence of molecular oxygen, the implanted C is unstable with respect to desorption of CO. These findings are also in agreement with the fact that implanted C atoms are not stable either when the temperature is raised, or in the presence of air. We also observe a strong C-surface vacancy interaction that stabilizes C atoms on the surface and on the other hand decreases the energy of vacancy formation. Such interaction is rationalized in terms of an electron shift from the Ti3d levels toward the partially occupied C 2p in-gap band states, according to a mechanism quite similar to that observed in N-doped surfaces. Finally, the analysis of the electronic structure suggests that the photocatalytic activity of rutile could be improved upon doping with C because of the presence of in-gap states that can be more or less occupied depending on the vacancy concentration.

Acknowledgment. This work was funded by the Ministerio de Ciencia e Innovación, MICINN, from Spain (Projects MAT2008-04918, CSD2008-00023), and the Junta de Andalucía (Project P08-FQM-03661). Y.O. gratefully acknowledges the MICINN for a predoctoral grant. We also thank the computational resources provided by the Barcelona Supercomputing Center−Centro Nacional de Supercomputación.

CM803436E